Available online at www.sciencedirect.com
SCIENCE DIRECT®
Journal of Sound and Vibration 281 (2005) 1207–1216
JOURNAL OF SOUND AND VIBRATION
www.elsevier.com/locate/jsvi

Short Communication

A simple finite difference scheme for modeling the finite-time blow-up of acoustic acceleration waves

P.M. Jordan[a,*], C.I. Christov[b]

[a]*Code 7181, Naval Research Laboratory, Stennis Space Center, MS 39529, USA*
[b]*Department of Mathematics, University of Louisiana at Lafayette, Lafayette, LA 70504, USA*

Received 7 January 2004; accepted 25 March 2004
Available online 5 November 2004

1. Introduction

The main purpose of this communication is to present a simple finite difference scheme that does an exceptionally good job of capturing the process by which an acoustic acceleration wave, defined as a propagating jump discontinuity in at least one of the first derivatives of the acoustic field variables, blows-up in finite time (see e.g., Ref. [1]).

Thomas [2] appears to have been the first to determine exact expressions describing the growth and/or decay of acceleration waves (or "sonic discontinuities" as they are referred to in Ref. [2]) in flows of inviscid ideal gases. Later, Coleman and Gurtin [3] studied the amplitude evolution of acceleration waves and mild discontinuities in fluids which exhibit mechanical dissipation via the relaxation of internal state variables. These authors went on to conjecture that acceleration wave blow-up implies that a shock wave, which is a propagating jump discontinuity in at least one of the acoustic field variables themselves, had in fact formed. They noted, however, that a rigorous mathematical proof of their supposition was lacking.

The scheme we develop here, which can be executed on a relatively inexpensive desktop or laptop computer, is tested on a nonlinear initial-boundary value problem (IBVP) which models acoustic acceleration wave propagation in an organ pipe. In addition to the numerical work, we also present an analytical analysis of this IBVP using singular surface theory and note possible

*Corresponding author. Tel.: +1-228-688-4338; fax: +1-228-688-5049.
E-mail address: pjordan@nrlssc.navy.mil (P.M. Jordan).

0022-460X/$ - see front matter
doi:10.1016/j.jsv.2004.03.067

extensions of this research. Our findings provide numerical support for the conjecture of Coleman and Gurtin [3] and show that a simple finite difference scheme can be used effectively in the numerical analysis of start-up flow problems which appear to exhibit discontinuity formation.

Before starting our analysis, it should be noted that the study of acceleration waves, which has applications in many areas of the physical sciences, has been a topic of much interest for over a century (see, e.g., Refs. [1,4,5] and the references therein). In particular, acceleration wave analysis has been, and remains, an important tool in theoretical investigations of the various formulations of thermoelasticity which have been proposed since the 1960s [5,6].

Let us begin by considering the (lossless) Lighthill–Westervelt (LW) equation in one spatial dimension [7–9]:

$$c_0^2\phi_{xx} - \phi_{tt} = c_0^{-2}\beta\{(\phi_t)^2\}_t, \quad \beta = \begin{cases} (\gamma+1)/2, & \text{gases;} \\ 1 + B/(2A), & \text{liquids;} \end{cases} \tag{1}$$

where $\phi = \phi(x,t)$ denotes the velocity (or acoustic) potential; x denotes the spatial (Cartesian) coordinate; t denotes time; c_0 is the sound speed associated with infinitesimal-amplitude acoustics ($c_0 = \sqrt{\gamma\wp_0/\varrho_0}$ in gases); $\beta(>1)$ is the coefficient of nonlinearity [10]; $\gamma = c_p/c_v$ is the adiabatic index ($\gamma > 1$); and where the constants c_p and c_v are the specific heats at constant pressure and volume, respectively. Here, $\mathfrak{U} = (u(x,t), 0, 0)$ is the velocity vector, where $u = \phi_x$, and we note that $\nabla \times \mathfrak{U}$ is identically zero, the ratio B/A is the nonlinearity parameter [10], and the positive constants $\wp_0$ and ϱ_0 denote the values of the thermodynamic pressure $\wp$ and mass density ϱ in the equilibrium state. (By equilibrium state we mean the unperturbed state in which $u = 0$, $\varrho = \varrho_0$, and $\wp = \wp_0$.)

The LW equation describes the homentropic propagation of planer acoustic waves in homogeneous, inviscid fluids under the finite-amplitude (i.e. small but finite Mach number) approximation. The origins of this PDE can be traced back to Lighthill's [11] 1952 paper on the process of aerodynamic sound generation, in which he stated what is know today as the Lighthill turbulence stress tensor for the acoustic field, and Westervelt's [12] 1963 work on highly directional transmitters and receivers in which he derived his well-known nonlinear equation for the acoustic pressure by neglecting the viscous contribution in the Lighthill turbulence stress tensor. Lastly, it should be noted that the LW equation, which is a special case of Kuznetsov's equation, also arises in the study of sound beams (again, see Refs. [7–9] and the references therein).

2. Acceleration waves and jump amplitudes

Clearly, the usual form of the LW equation, i.e., the form given in Eq. (1), is not well suited for the analysis of acceleration waves. Hence, for the purposes of the present Letter we make use of the relations $u = \phi_x$ and $\rho = -\varrho_0 c_0^{-2}\phi_t$, where $\rho = \varrho - \varrho_0$ is the acoustic density ($|\rho| \ll \varrho_0$), and recast Eq. (1) as the first-order system

$$u_t + \varrho_0^{-1}c_0^2\rho_x = 0, \quad \rho_t + \varrho_0(1 - 2\beta\rho/\varrho_0)^{-1}u_x = 0, \tag{2}$$

where the eigenvalues of the coefficient matrix of this system are given by $\lambda_{1,2} = \pm c_0(1 - 2\beta\rho/\varrho_0)^{-1/2}$ and we note that $\rho < \varrho_0/(2\beta)$ under the finite-amplitude approximation. Now, since

$\lambda_{1,2} \in \mathbb{R}$ and $\lambda_1 \neq \lambda_2$, it follows that these equations comprise a strictly hyperbolic system [13]. Consequently, it is clear that discontinuities in the first derivatives of u and ρ must propagate along the system's characteristic curves.

Imagine now a smooth planer surface $x = \Sigma(t)$ propagating along the x-axis of a Cartesian coordinate system into a region $\mathscr{R}$ filled with a fluid described by the LW equation, the speed of Σ with respect to the fluid being $|U|(\neq 0)$. Suppose that $u, \rho \in C(\mathscr{D}_1)$, where $\mathscr{D}_1 = \{(x,t) : x \in \mathscr{R}, t \in \mathbb{R}\}$, and $u, \rho \in C^2(\mathscr{D}_2)$, where $\mathscr{D}_2 = \{(x,t) : x \in (\mathscr{R} \backslash \Sigma), t \in \mathbb{R}\}$, but that at least one of the first derivatives of u or ρ, say u_t, suffers a jump discontinuity (or jump) on crossing Σ; i.e., $[u] = [\rho] = 0$ but $[u_t] \neq 0$, where the amplitude of the jump in a function $F = F(x,t)$ across Σ is defined as

$$[F] \equiv F^- - F^+, \tag{3}$$

and where $F^{\mp} \equiv \lim_{x \to \Sigma(t)^{\mp}} F(x,t)$ are assumed to exist. (Employing the usual notation, a "+" superscript corresponds to the region into which Σ is advancing while a "−" superscript corresponds to the region behind Σ.) Such a surface, which is singular with respect to u_t, is known as an acceleration wave [1]. Hence, assuming that the value of $[u_t]$ at $t = 0$ is known, we proceed to determine the value of $[u_t]$ for all $t > 0$.

The first step in the process is employing Hadamard's lemma [1,3,6]

$$\frac{\mathrm{d}[F]}{\mathrm{d}t} = [F_t] + U[F_x], \tag{4}$$

where $\mathrm{d}/\mathrm{d}t$ is the (one-dimensional) displacement derivative with respect to Σ (i.e., the time-rate-of-change measured by an observer traveling with Σ), along with the fact that $[u] = [\rho] = 0$, to obtain the jump relations

$$U[u_x] + [u_t] = 0, \quad U[\rho_x] + [\rho_t] = 0. \tag{5}$$

If we assume that the fluid ahead of the acceleration wave (i.e., the fluid in the region which Σ is moving into) is in its equilibrium state ($\Rightarrow \varrho^+ = \varrho_0$), then it is clear that $\rho^+ = 0$. As a result, it is not difficult to show, using once again the fact that $[\rho] = 0$ along with the formula for the jump of a product [6],

$$[FG] = F^+[G] + G^+[F] + [F][G] \tag{6}$$

that

$$[\rho \rho_t] = 0. \tag{7}$$

On taking the jumps of Eqs. (2), which is permissible since they hold on both sides of Σ, and using Eq. (7), we get the other two jump relations

$$[u_t] + \varrho_0^{-1} c_0^2 [\rho_x] = 0, \quad \varrho_0 [u_x] + [\rho_t] = 0. \tag{8}$$

Our next step is to determine U. To this end, we set the determinant of the coefficient matrix of this system of (four) jumps equations to zero. This leads to the propagation condition $U^2 - c_0^2 = 0$, and consequently the solutions $U = \pm c_0$. However, since Eq. (1) is invariant under the transformation $x \to -x$, it is clear that we need only consider, without loss of generality, a right-traveling acceleration wave (i.e., the positive solution) and it follows that the acceleration wave corresponds to the moving plane $\Sigma(t) = c_0 t$, where $\Sigma(0) = 0$ is assumed.

Although we omit the remaining details, it is a straightforward process using Hadamard's lemma, Eqs. (2), and the jump relations given above to derive the following nonlinear, ordinary

differential equation [3]:

$$\frac{\mathrm{d}a}{\mathrm{d}t} - \beta c_0^{-1} a^2 = 0, \tag{9}$$

where $a(t) \equiv [u_t]$. Eq. (9) governs the temporal evolution of the jump amplitude $a(t)$; it is a reduced form of the well-known Bernoulli equation and its exact solution is given by

$$a(t) = \frac{a(0)}{1 - t\beta c_0^{-1} a(0)}, \tag{10}$$

where $a(0) \equiv [u_t]_0$ and where $[u_t]_0$ denotes the value of $[u_t]$ at $t = 0$. From Eq. (10) we observe that if $a(0) > 0$ then $a(t) \to \infty$ as $t \to \dagger_\infty$, where the breakdown time $\dagger_\infty$ is given by

$$\dagger_\infty \equiv \frac{c_0}{\beta a(0)}, \tag{11}$$

i.e., $a(t)$ blows up at $t = \dagger_\infty$. In contrast, if $a(0) < 0$ then $\dagger_\infty < 0$ as well, a reflection of the fact that $a(t)$ is always bounded when $a(0) < 0$. More precisely, if $a(0) < 0$ then $a(t) \to 0 - 0$ monotonically as $t \to \infty$, an example of what has been termed an "exceptional case" [4].

Lastly, we use the relation $p = c_0^2 \rho$, where $p = \wp - \wp_0$ is the acoustic pressure, and Eqs. (8) to derive the following expressions for the jumps in the first derivatives of p:

$$[p_t] = -\varrho_0 c_0^2 [u_x] = c_0^2 [\rho_t], \quad [p_x] = -\varrho_0 [u_t] = c_0^2 [\rho_x]. \tag{12}$$

From Eqs. (5) and (12) it is evident that if either of the first derivatives of any one of the acoustic field variables suffers a jump across Σ, then so do the other five and, since U is a constant, it is clear that every jump amplitude is directly proportional to all the others. Thus, we see that $a(t)$ can easily be expressed in terms of $[u_x]$ or the jumps in either of the first derivatives ρ or p.

3. Problem statement and mathematical formulation

Let us now turn our attention to the problem of finite amplitude acoustic waves propagating in an organ pipe of length ℓ. Initially, the air inside, which we assume behaves essentially like a diatomic ideal gas, is in its equilibrium state. Let the pipe occupy the open interval $(0, \ell)$ along the x-axis and let the pipe's end at $x = \ell$ be open to the atmosphere. At time $t = 0$, a sinusoidal signal of magnitude and frequency ϱ_m and Ω, respectively, is suddenly inserted at the end $x = 0$ and maintained for all $t > 0$. Considering both the $\mp\varrho_\mathrm{m}$ cases, we wish to determine the acoustic pressure, density, etc. inside the pipe for all $0 < t < |\dagger_\infty|$.

The mathematical formulation of this unsteady compressible flow consists of the following IBVP involving the LW equation, which we formulate in terms of the acoustic density using the relation $\rho = -\varrho_0 c_0^{-2} \phi_t$:

$$c_0^2 \rho_{xx} - \rho_{tt} = -\varrho_0^{-1} \beta (\rho^2)_{tt}, \quad (x, t) \in (0, \ell) \times (-\infty, |\dagger_\infty|); \tag{13a}$$

$$\varrho(0, t) = \varrho_0 \mp \varrho_\mathrm{m} H(t) \sin[\Omega t], \quad \varrho(\ell, t) = \varrho_0, \quad t < |\dagger_\infty|; \tag{13b}$$

$$\varrho(x, 0) = \varrho_0, \quad \varrho_t(x, 0) = 0, \quad x \in (0, \ell); \tag{13c}$$

where $H(\cdot)$ denotes the Heaviside unit step function and $\varrho_{\mathrm{m}}(\ll\varrho_0)$ and Ω are positive constants. (For a discussion detailing other aspects of finite amplitude acoustic phenomena in organ pipes, see Ockendon and Ockendon [14] and the references therein.) Employing the nondimensional variables

$$\phi' = \phi/(\ell V), \quad x' = x/\ell, \quad t' = tc_0/\ell, \quad u' = u/V, \quad p' = \rho/\varrho_{\mathrm{m}} = \rho/(\varepsilon\varrho_0), \tag{14}$$

where $V = c_0\varrho_{\mathrm{m}}/\varrho_0$ is a characteristic flow speed and $\varepsilon = V/c_0$ denotes the Mach number, we recast IBVP (13) in terms of the dimensionless acoustic pressure as

$$p_{xx} - (1 - 2\varepsilon\beta p)p_{tt} = -2\varepsilon\beta(p_t)^2, \quad (x,t) \in (0,1) \times (-\infty, |t_\infty|); \tag{15a}$$

$$p(0,t) = (-1)^{n+1}\mathrm{H}(t)\sin[\omega t], \quad p(1,t) = 0, \quad t < |t_\infty|; \tag{15b}$$

$$p(x,0) = 0, \quad p_t(x,0) = 0, \quad x \in (0,1); \tag{15c}$$

where $\omega = \Omega(\ell/c_0)$ is the dimensionless frequency; t_∞ denotes the dimensionless form of $\dagger_\infty$; $n = 0, 1$ as demanded; we have expanded the second derivative term on the RHS of Eq. (13a) and simplified; and all primes are suppressed but understood. Based on the results given in Section 2, we find that in the case of IBVP (15), the (dimensionless) jump amplitude and breakdown time are given by

$$[p_x] = -[p_t] = \frac{\omega(-1)^n}{1 + \varepsilon\beta\omega t(-1)^n} \quad \text{and} \quad t_\infty \equiv \frac{(-1)^{n+1}}{\varepsilon\beta\omega}. \tag{16}$$

Here, the amplitude of the jump in the time-derivative of the boundary condition at $x = 0$ across the plane $t = 0$ is $[p_t]_0 = \omega(-1)^{n+1}$, where

$$[p_t]_0 \equiv \omega(-1)^{n+1}\left\{\lim_{t\to 0+0} H(t)\cos[\omega t] - \lim_{t\to 0-0} H(t)\cos[\omega t]\right\} = \omega(-1)^{n+1}\lim_{t\to 0+0}\cos[\omega t], \tag{17}$$

we observe that (see e.g., Ref. [1])

$$n = \begin{cases} 0 & \Rightarrow \text{Expansive acceleration wave,} \\ 1 & \Rightarrow \text{Compressive acceleration wave,} \end{cases} \tag{18}$$

and we note that c_0 has been normalized to unity under the set of dimensionless variables employed. In addition, we observe that if $n = 0$ (resp. $n = 1$), then $t_\infty < 0$ (resp. $t_\infty > 0$). Thus, it is clear that only if the acceleration wave is compressive will the jumps in the first derivatives of p blow-up, and do so in finite time $t = t_\infty$ [2,3].

In the linearized case of IBVP (15), corresponding to setting $\varepsilon \equiv 0$, Eq. (15a) reduces to the wave equation $p_{xx} - p_{tt} = 0$ and the corresponding exact solution can be easily found using the Laplace transform. For the purposes of the present communication, however, the following simple expression, which very closely approximates the former for $t \in (0,1)$, will be adequate:

$$p(x,t) \approx (-1)^{n+1}H(t-x)\sin[\omega(t-x)] \quad \text{(Linearized case).} \tag{19}$$

4. Scheme construction and numerical verification

Having stated the IBVP and determined the corresponding jump amplitude and breakdown time, we are now ready to make use of the finite-difference method to obtain a numerical solution. Specifically, we construct a simple, but surprisingly effective, finite-difference scheme that does an extremely good job capturing the "shocking-up" behavior described above. Also, to simplify our presentation let us limit our attention to the acceleration wave's initial passage through the organ pipe, so as to avoid having to deal with changes in the waveforms due to reflection, and require that $|t_\infty|$ correspond to the time of first reflection, i.e., $|t_\infty| = 1$.

To this end, IBVP (15) must be discretized. The first step in this process is selecting the integers $M \geqslant 2$ and $K \geqslant 2$. Next, we set $\Delta x = T/M$ and $\Delta t = T/K$, where Δx and Δt, respectively, denote the (uniform) spatial- and temporal-step sizes and $T \in (0, 1]$ denotes the supremum of t value for which the solution is sought. (We recall that in terms of the dimensionless variables $U = 1$.) It then follows that the mesh points (x_m, t_k) are given by $x_m = m(\Delta x)$, for each $m = 0, 1, \ldots, M$, and $t_k = k(\Delta t)$, for each $k = 0, 1, \ldots, K$. The third step involves the discretization of Eq. (15a). The simplest way to accomplish this is by replacing the second-order derivatives with centered-difference quotients and $(p_t)^2$ with a backwards-Euler quotient squared. Making these replacements yields the difference equation

$$\frac{p_{m+1}^k - 2p_m^k + p_{m-1}^k}{(\Delta x)^2} - (1 - 2\varepsilon\beta p_m^k)\left(\frac{p_m^{k+1} - 2p_m^k + p_m^{k-1}}{(\Delta t)^2}\right) = -2\varepsilon\beta\left(\frac{p_m^k - p_m^{k-1}}{\Delta t}\right)^2, \tag{20}$$

where $p_m^k \approx p(x_m, t_k)$. Now, since this scheme is linear in the most advanced time-step approximation p_m^{k+1}, we can solve for this term to obtain, after some manipulation, the explicit scheme:

$$p_m^{k+1} = \frac{R^2\{p_{m+1}^k - 2p_m^k + p_{m-1}^k\} + (1 - 2\varepsilon\beta p_m^k)\{2p_m^k - p_m^{k-1}\} + 2\varepsilon\beta\{p_m^k - p_m^{k-1}\}^2}{1 - 2\varepsilon\beta p_m^k}, \tag{21}$$

where $R = (\Delta t)/(\Delta x)$. Here, we observe that Eq. (21) holds for each $m = 1, 2, \ldots, M - 1$ and $k = 1, 2, \ldots, K - 1$ and that the overall truncation error of the scheme is $\mathcal{O}[(\Delta x)^2 + (\Delta t)]$. The last step concerns discretizing the boundary conditions and initial conditions. This is a relatively simple process and we refer the reader to, e.g., Burden and Faires [15] for details.

For air at 20 °C we have $\gamma = 1.402$ ($\Rightarrow \beta = 1.201$) and $c_0 = 343\,\mathrm{m/s}$ (see Appendix 10, Table (c), of Ref. [16]). For simplicity, we took $\omega = \pi$, giving a dimensional frequency of $\Omega = (343\pi/\ell)\,\mathrm{Hz}$. Consequently, the Mach number required to give $|t_\infty| = 1$ is found to be $\varepsilon \approx 0.265$. While this value of ε may be a bit large, considering the finite-amplitude requirement $\varepsilon \ll 1$, it does, in fact, place the flow well within range where compressibility effects are becoming important (i.e., where the incompressibility approximation is not valid [17]) and, as we will soon see, provides for clearly distinguishable plots of the nonlinear vs. linear solution curves.

In order to ascertain the scheme's stability limits, we first conducted an exhaustive series of numerical experiments (not presented here) that involved varying R between zero and one with β, ε, and ω assigned the values noted above. What we found was that for $R > 1/2$, rapid progression to instability occurred, while for $R \leqslant 1/2$ the actual numerical value of R had quantitatively little impact on the results. We thus concluded that to ensure the stability of our (explicit) scheme, the

condition $R \leqslant 1/2$ had be satisfied. Consequently, given that the numerical output is essentially independent of R for $R \leqslant 1/2$, we choose $R = 1/2$ since it requires the fewest number of time steps to reach a given time stage.

To illustrate both the efficacy of our scheme and the apparent transition from acceleration to shock wave, we have, in Figs. 1 and 2, plotted the acoustic pressure profile corresponding to IBVP (15). Specifically, the time-sequences shown in Figs. 1 and 2, respectively, illustrate the evolution of the $|p|$ vs. x and the p vs. x solution profiles during the acceleration wave's initial transit of the pipe, with the former and latter respectively corresponding to the cases $n = 0, 1$. The curves shown in bold, which correspond to IBVP (15) with $\varepsilon\beta \approx (0.265)(1.201) \approx 0.318$, were produced from data sets computed by a simple algorithm which implemented our scheme on a PC running the software package *Mathematica* (Version 5.0). Interpolations between the points were then accomplished using *Mathematica's* built-in cubic splin routine. To help illustrate the decay and growth of the acceleration wave amplitudes, we have included the tangents to the solution profiles at $x = t$, which are plotted from Eq. $(16)_1$ as broken line segments. And to allow for comparisons of the nonlinear vs. linear versions of IBVP (15), we have also graphed the approximate linearized solution given in Eq. (19) as the thin-solid curves.

Now, since we are considering lossless flow, no attenuation of any other kind of the waveform is present. This means that during the initial passage, the maximal amplitude of the solution profile

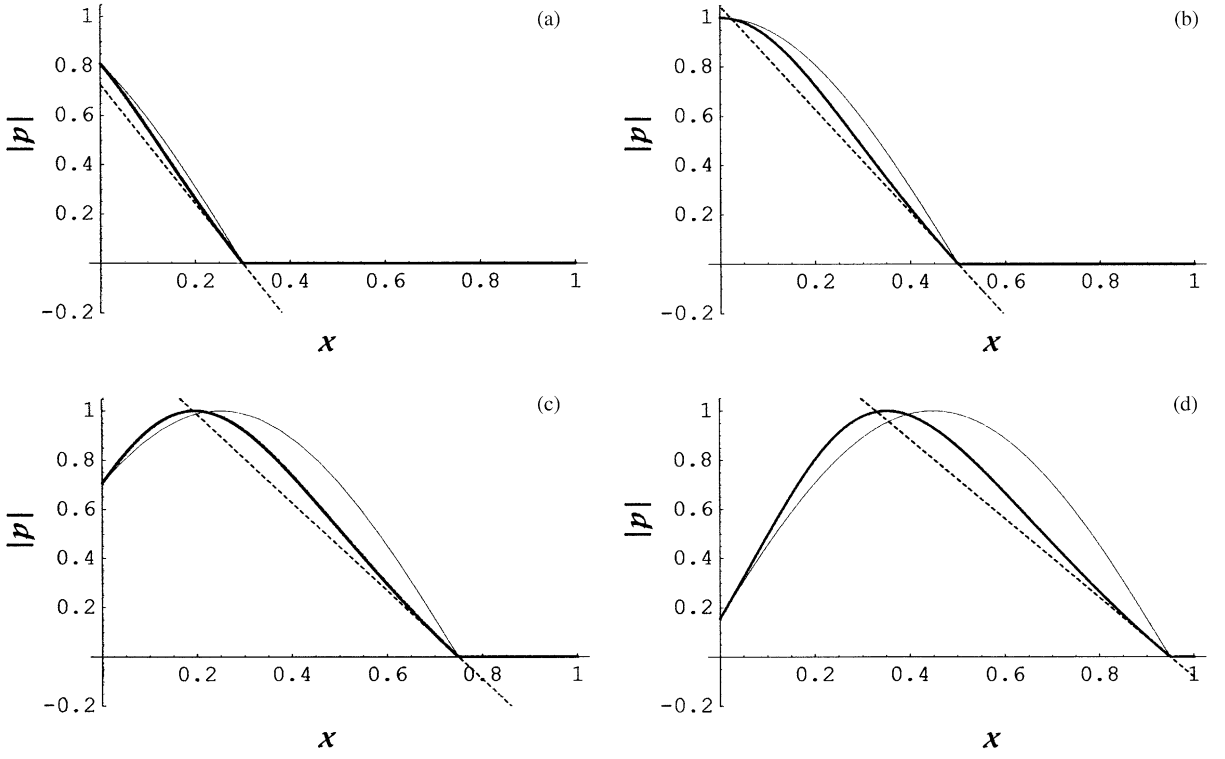

Fig. 1. $|p|$ vs. x with $n = 0$, $\omega = \pi$, $t_\infty = -1$, $T = 1$, $\Delta x = 5.0 \times 10^{-4}$, $\Delta t = 2.5 \times 10^{-4}$, and $R = 1/2$. Bold: $\varepsilon\beta \approx 0.318$. Broken: tangent line to bold profile at $x = t$. Thin-solid: Eq. (19). (a) $t = 0.30$, (b) $t = 0.50$, (c) $t = 0.75$, (d) $t = 0.95$.

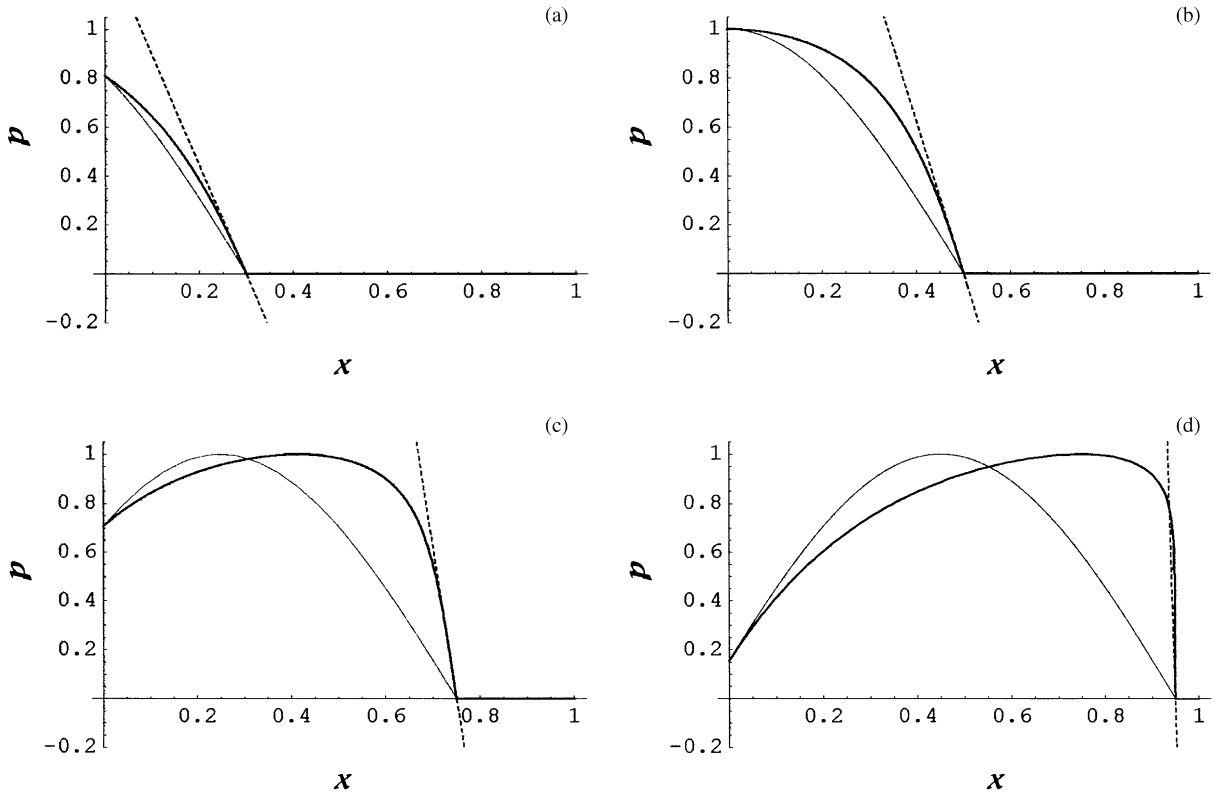

Fig. 2. p vs. x with $n = 1$, $\omega = \pi$, $t_\infty = 1$, and $R = 1/2$. For $t = 0.30$, 0.5, 0.75: $T = 1$, $\Delta x = 5.0 \times 10^{-4}$, and $\Delta t = 2.5 \times 10^{-4}$. For $t = 0.95$: $T = 0.95$, $\Delta x = 7.6 \times 10^{-5}$, $\Delta t = 3.8 \times 10^{-5}$. Bold: $\varepsilon\beta \approx 0.318$. Broken: tangent line to bold profile at $x = t$. Thin-solid: Eq. (19). (a) $t = 0.30$, (b) $t = 0.50$, (c) $t = 0.75$, (d) $t = 0.95$.

should be equal to the maximal value of the input signal. Figs. 1 and 2 clearly confirms this theoretical prediction, indicating unequivocally that our scheme does not introduce appreciable artificial (i.e., numerically induced) dissipation or gain. Further, Figs. 1 and 2 also make clear that our scheme captures the fact that the acceleration wave's propagation speed is exactly unity as witnessed by the comparison of the linear (thin-solid) and nonlinear (bold) profiles. Moreover, as Fig. 2 indicates, all the above-mentioned results obtained are valid rather close to the instant when $t = t_\infty$, which additionally strengthens our confidence in the scheme developed here.

Lastly, it should be mentioned that we also tested several second order in time schemes for the first-order time derivative that enters the nonlinear term, e.g., the standard one-side three-stage difference representation of the derivative p_t. Unfortunately, given the same physical/scheme parameters, the results obtained were invariably worse than those for our simple scheme given in Eq. (21). In fact, even a Richardson extrapolation did not really do a good job because it enhanced the spurious part of the solution instead of damping it. This last finding we attribute to the hyperbolic nature of the LW equation.

5. Summary and final remarks

We have presented a simple, but very effective, finite difference scheme to numerically solve the LW equation in the context of IBVP (15). Using it, we were able to provide a numerical justification of the conjecture made by Coleman and Gurtin [3] regarding the connection between acceleration wave blow-up and shock wave formation in finite time t_∞. Another important result is that our scheme gives not just a qualitative, but also a very good quantitative description of the solution profile corresponding to $n = 1$ as it rapidly steepens (i.e., as it shocks-up). This point is very well illustrated in Fig. 2. Here, we see that the magnitude of the slope of the tangent line, which is given by $|[p_x]| = |p_x^-|$, is tending to infinity as the acceleration wave nears $x = 1$.

In particular, with $n = 1$our scheme is able to accurately capture 95% of the wave's evolution before the first reflection. In fact, the solution profiles generated by our scheme are stable and of high accuracy, for both the $n = 0, 1$ cases, and they are very smooth except for the well-defined corners corresponding to the two acceleration waves. The behavior shown is qualitatively and quantitatively in very good/excellent agreement with the analytical predictions of the flow's behavior given in Section 3. Naturally, with the increase of t beyond 0.95, the $n = 1$ case begins to exhibit instability in the vicinity of the profile's crest and around the discontinuity (i.e., shock) that appears to be forming (again, see Fig. 2).

The logical extension of the physical scope of the present work would be to numerically investigate the propagation of nonlinear acoustic acceleration waves in media that are not necessarily in the equilibrium state. Further extensions could include adapting our scheme to simulate singular surface phenomena which occur in other areas of the physical sciences, most notably some of the modern formulations of thermoelasticity [5,6].

Finally, regarding the further development and refinement of the numerical scheme, future versions could include nonuniform spatial grids and adaptive time steps for better resolution as $t \to t_\infty$, as well as the use of conservative [18,19] and/or nonstandard [20,21] finite-differencing methods.

Acknowledgements

The first author was supported by ONR/NRL funding (PE 061153N).

References

[1] P.J. Chen, Growth and decay of waves in solids, in: S. Flügge (Ed.), *Handbuch der Physik*, VIa/3, Springer, Berlin, 1973, pp. 303–402.

[2] T.Y. Thomas, The growth and decay of sonic discontinuities in ideal gases, *Journal of Mathematics and Mechanics* 6 (1957) 455–469.

[3] B.D. Coleman, M.E. Gurtin, Growth and decay of discontinuities in fluids with internal state variables, *Physics of Fluids* 10 (1967) 1454–1458.

[4] W.F. Ames, Discontinuity formation in solutions of homogeneous non-linear hyperbolic equations possessing smooth initial data, *International Journal of Non-Linear Mechanics* 5 (1970) 605–615.

[5] R. Quintanilla, B. Straughan, A note on discontinuity waves in type III thermoelasticity, Proceedings of the Royal Society of London A460 (2004) 1169–1175.
[6] K.A. Lindsay, B. Straughan, Temperature waves in a rigid heat conductor, *Journal of Applied Mathematics and Physics (ZAMP)* 27 (1976) 653–662.
[7] F. Coulouvrat, On the equations of nonlinear acoustics, *Journal de Acoustique* 5 (1992) 321–359.
[8] S. Makarov, M. Ochmann, Nonlinear and thermoviscous phenomena in acoustics. II, *Acustica* 83 (1997) 197–222.
[9] K. Naugolnykh, L. Ostrovsky, *Nonlinear Wave Processes in Acoustics*, Cambridge University Press, New York, 1998.
[10] R.T. Beyer, The parameter B/A, in: M.F. Hamilton, D.T. Blackstock (Eds.), *Nonlinear Acoustics*, Academic Press, New York, 1997, pp. 25–39.
[11] M.J. Lighthill, On sound generated aerodynamically I. General theory, *Proceedings of the Royal Society of London* A 211 (1952) 564–587.
[12] P.J. Westervelt, Parametric acoustic array, *Journal of the Acoustical Society of America* 35 (1963) 535–537.
[13] J.D. Logan, *An Introduction to Nonlinear Partial Differential Equations*, Wiley, New York, 1994, pp. 227–232.
[14] H. Ockendon, J.R. Ockendon, Nonlinearity in fluid resonances, *Meccanica* 36 (2001) 297–321.
[15] R.L. Burden, J.D. Faires, *Numerical Analysis*, fifth edition, PSW-Kent, Boston, MA, 1993.
[16] L.E. Kinsler, et al., *Fundamentals of Acoustics*, third edition, Wiley, New York, 1982.
[17] J.A. Liggett, *Fluid Mechanics*, McGraw-Hill, New York, 1994, p. 64.
[18] C.I. Christov, G. Nicolis, Spatio-temporal chaos and intermittency in a 1-dimensional energy-conserving coupled maps lattice, *Physica* A 228 (1995) 326–342.
[19] C.I. Christov, An energy-consistent Galilean-invariant dispersive shallow-water model, *Wave Motion* 34 (2001) 161–174.
[20] R.E. Mickens, A.B. Gumel, Construction and analysis of a nonstandard finite difference scheme for the Burgers–Fisher equation, *Journal of Sound and Vibration* 257 (2002) 791–797.
[21] R.E. Mickens, P.M. Jordan, A positivity-preserving nonstandard finite difference scheme for the damped wave equation, *Numerical Methods for Partial Differential Equations* 20 (2004) 639–649.